

Learning Constrained Dynamics with Gauss' Principle adhering Gaussian Processes

A. René Geist[†]

GEIST@IS.MPG.DE

Sebastian Trimpe[†]

TRIMPE@IS.MPG.DE

[†] Intelligent Control Systems Group, Max Planck Institute for Intelligent Systems

Editors: A. Bayen, A. Jadbabaie, G. J. Pappas, P. Parrilo, B. Recht, C. Tomlin, M. Zellinger

Abstract

The identification of the constrained dynamics of mechanical systems is often challenging. Learning methods promise to ease an analytical analysis, but require considerable amounts of data for training. We propose to combine insights from analytical mechanics with Gaussian process regression to improve the model's data efficiency and constraint integrity. The result is a Gaussian process model that incorporates a priori constraint knowledge such that its predictions adhere to Gauss' principle of least constraint. In return, predictions of the system's acceleration naturally respect potentially non-ideal (non-)holonomic equality constraints. As corollary results, our model enables to infer the acceleration of the unconstrained system from data of the constrained system and enables knowledge transfer between differing constraint configurations.

Keywords: Constrained Lagrangian systems, Gauss' Principle, Gaussian Processes, Nonlinear system identification, Structured learning, Transfer learning

1. Introduction

The acquisition of accurate models of dynamical systems is essential for a multitude of engineering applications. If the function generating the data is unknown or too complex to be modelled from first principles, non-parametric learning models aim at inferring a function solely from the data. Gaussian Processes (GPs) are non-parametric and have been commonly used to learn dynamics. They have demonstrated their versatility in approximating continuous nonlinear functions on a plethora of real-world problems (Rasmussen and Williams, 2006), including modeling of dynamical systems (Nguyen-Tuong and Peters, 2011; Kocijan et al., 2005; Frigola et al., 2013; Mattos et al., 2016; Doerr et al., 2017; Eleftheriadis et al., 2017; Doerr et al., 2018). In this context, GPs are often preferred over alternative methods, since they provide a measure of the uncertainty about function estimates in the form of the posterior variance. Additionally, they allow for the incorporation of various model assumptions through the covariance function (kernel). However, data on real-world systems is often scarce and contains only partial information, which is why training purely data-driven models to sufficient prediction accuracy is challenging. Further, predictions made by standard GP models may violate critical system constraints compromising the predictions' integrity.

A promising approach to improve the data efficiency and constraint integrity of a GP model involves the incorporation of a priori available *structural knowledge* in the design of the covariance function. Turning to mechanical systems, the identification of fundamental structural relationships has been studied intensively by scholars for the last two centuries under the subject of analytical mechanics. In this work, we leverage the structure inherent in holonomic and non-holonomic con-

straint equations, which also can be non-ideal. For example, a pendulum’s rod or a rolling wheel enforce a holonomic or non-holonomic constraint, respectively. A constraint is referred to as being *non-ideal* if it induces forces onto the system that produce virtual work (e.g., damping and friction), and it is called *ideal* if no virtual work is produced (e.g., pendulum rod). The constrained dynamics of such systems are described by the Udwadia-Kalaba equation (UKE) (Udwadia and Kalaba, 1992, 2007). The UKE is a direct result of *Gauss’ principle* of least constraint (Gauß, 1829), which states that a system’s constrained acceleration can be cast as the solution of a least-squares problem.

In this work, we propose a GP model that leverages mechanical constraints as prior knowledge for learning dynamics of mechanical systems. Specifically, a GP is transformed by constraint equations to satisfy Gauss Principle. The resulting *Gauss’ Principle adhering Gaussian Process* (GP²) performs inference in a physically substantiated sub-space of the acceleration space. In return, the data-efficiency and physical integrity are improved compared to the untransformed GP.

2. Problem Formulation

The acceleration of constrained mechanical rigid-body systems is described as

$$\ddot{q} = h(q, \dot{q}, t) = M^{-1}(q, t)F(q, \dot{q}, t), \quad h : \mathbb{R}^D \rightarrow \mathbb{R}^n \quad (1)$$

with state dimension n , $D = 2n + 1$, symmetric positive definite matrix $M(q, t)$, and vector $F(q, \dot{q}, t)$. The variables q , \dot{q} , \ddot{q} correspond to the system’s positions, velocities, and accelerations, respectively. Although they depend on time t , we generally omit the time dependence for these and other variables if this is clear from the context. Inhere, the system is solely subject to constraint forces arising from sufficiently smooth (*non-)*holonomic constraints, $c_i(q, \dot{q}, t, \theta_p) = 0$, with $i = 1, 2, \dots, m$, whose (second) time-derivatives are linear in \ddot{q} , yielding

$$A(q, \dot{q}, t)\ddot{q} = b(q, \dot{q}, t), \quad (2)$$

with functions $A : \mathbb{R}^D \rightarrow \mathbb{R}^{m \times n}$, $b : \mathbb{R}^D \rightarrow \mathbb{R}^m$, and $m < n$. We refer to (2) as the *constraining equation*. Most applications of analytical mechanics deal with such constraints (Udwadia and Kalaba, 2007, p. 80). These constraints can be *non-ideal*, but naturally must be consistent.

Further, it is assumed that the parametric functions $\{A, b, M\}$ are known, e.g., from a preceding mechanical analysis of the “unconstrained” rigid-body dynamics (see Section 4), while the system’s parameters $\theta_p = [p_1, \dots, p_r]$ are potentially unknown. For the above-defined system, data $\mathcal{D} = \{x_k, y_k\}_{k=1}^N$ is available, consisting of input points $x_k = [q_k, \dot{q}_k, t_k]^\top$ and observations $y_k = h(x_k) + \epsilon_k$ where $y_k \in \mathbb{R}^n$ with ϵ_k denoting zero-mean Gaussian noise. In some cases, x_k includes a vector of control forces $u_k \in \mathbb{R}^{n_u}$ explicitly. While more general settings such as hidden states can be addressed in GP dynamics learning (Doerr et al., 2018), we here focus on the standard GP regression setting with noiseless inputs and noisy targets.

The main objective of this work is to learn h via a GP $\hat{h} \sim \mathcal{GP}(\mu_{\hat{h}}, K_{\hat{h}})$ that incorporates the structural knowledge $\{A, b, M\}$ in the GP’s mean $\mu_{\hat{h}}(x|\theta_p)$ and covariance function $K_{\hat{h}}(x, x'|\theta_p)$ such that its posterior mean approximates (1) while satisfying (2) exactly.

3. Related Work

We categorize related literature into the following aspects: (i) leveraging functional relations arising from analytical mechanics to structure learning; (ii) constructing GP kernels using semi-parametric models; and (iii) using linear transformations to provide structure to GP models.

The incorporation of functional relationships arising from the field of analytical mechanics starts gaining attention. For example, (Ledezma and Haddadin, 2018) use the recursive nature of the Newton-Euler equations of open-chain rigid-body configurations to derive a parametric regression model. Recently, (Lutter et al., 2018) detailed the direct incorporation of the Lagrange equations describing the inverse dynamics of holonomic ideal constrained systems into neural networks. Further, (Greydanus et al., 2019) combined Hamiltonian mechanics with neural networks to predict the forward dynamics of conservative mechanical systems. Our work is linked to (Cheng and Huang, 2015), in which the operators underlying the Lagrange equations are used to derive kernels which capture inverse dynamics as the Lagrangians projection. In comparison, our model builds on projection operations underlying mechanical constraint equations to enable structured learning of forward dynamics on possibly non-holonomic and non-ideally constrained systems.

If a parametric function is cast as a (Bayesian) linear regression problem, a degenerate GP covariance function can be derived to model the function non-parametrically. This relationship is used in (Nguyen-Tuong and Peters, 2010) to derive a structured GP kernel for learning the inverse dynamics of open-chain robot arms. In our work, we do not assume that the dynamics are linear in the system parameters, but instead, leverage that (2) is linear with respect to \ddot{q} .

Because GPs are closed under linear operations, and linear operators commonly occur in physical equations, such operators play a particularly important role in structured learning with GPs. Linear operations commonly used in literature are, *e.g.*, differentiation (Solak et al., 2003), integration, and wrapping of the GP inputs into a nonlinear function (Calandra et al., 2016). Furthermore, one particular application of GP regression revolves around efficiently learning the solution of differential equations by transforming GPs through convolution operators (Alvarez et al., 2009; Särkkä, 2011). (Jidling et al., 2017; Lange-Hegermann, 2018) discuss how to construct a GP kernel such that its realizations $f(x)$ fulfill a constrained equation of the form $A_x f(x) = 0$, where A_x is a linear operator. While our work also transforms a GP such that its predictions lie in a linear operator’s nullspace, we emphasize that in classical mechanics such operators enable the construction of a GP whose predictions satisfy nonlinear constraints in a physically meaningful manner. In comparison, the work in (Agrell, 2019) considers modeling a GP to fulfill an inequality constraint of the form $A_x f(x) \leq b(x)$ by conditioning its posterior on carefully selected virtual observations of $b(x)$. In contrast to (Jidling et al., 2017; Lange-Hegermann, 2018) and this work, (Agrell, 2019) ensures constraint satisfaction with a certain probability at selected sample points, while we ensure constraint satisfaction over the whole input range.

None of the above works addresses the problem of constrained modeling of rigid-body mechanical systems through a tailored GP satisfying an affine equality constraint as stated in Section 2.

4. Constrained Dynamics with Gauss’ Principle

In this section, we present a description of constrained mechanical systems that gives an explicit form for the constraint forces acting on a system as a function of the state x and constraining equation (2) as detailed in (Udwadia and Kalaba, 2002) and Sec. S3 and S4 of the supplementary material. This allows us in the following section to construct a GP that respects the constraints underlying (2).

We consider mechanical systems where a force F_a acting on rigid bodies results in the *unconstrained acceleration*

$$a = M(q, t)^{-1} F_a(x). \quad (3)$$

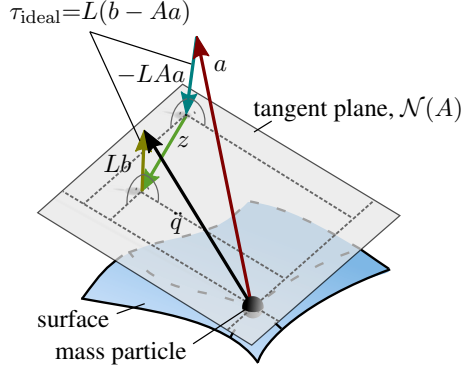


Figure 1: Mass particle sliding on a surface subject to Gauss' principle.

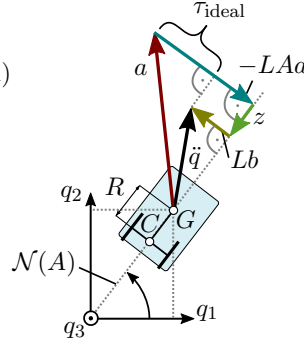


Figure 2: Unicycle subject to Gauss' Principle.

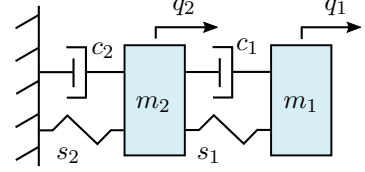


Figure 3: Duffing oscillator.

The term “unconstrained” refers to $a(x)$ describing potentially constrained Lagrangian dynamics onto which an (additional) constraining equation (2) has not yet been applied. If an (additional) constraint acts on the system, its movement changes to the *constrained acceleration* $\ddot{q} = a + \tau$. We refer to the term $\tau = \tau_{\text{ideal}} + z$ as the *constraining acceleration*, where $z(x)$ denotes the non-ideal part of $\tau(x)$ (e.g., damping and friction). Udwardia et al. (1997) refers to a constraining acceleration as non-ideal if it lies in the nullspace of $A(x)$, writing $\mathcal{N}(A)$, and as ideal if it lies in the range space of $A(x)$. Gauß (1829) observed that the *ideal constraining acceleration* $\tau_{\text{ideal}}(x)$ minimizes the functional $G(x) = \tau_{\text{ideal}}^T M \tau_{\text{ideal}}$. This fundamental principle underlying the constrained motion of rigid-body systems is referred to as *Gauss' principle of least constraint*. The minimizing solution of this least-squares problem is given by the UKE – omitting the dependencies on x for clarity – as

$$\ddot{q} = \underbrace{M^{-1} A^T (A M^{-1} A^T)^+}_{L(x, \theta_p)} b + \underbrace{(I - M^{-1} A^T (A M^{-1} A^T)^+ A)}_{T(x, \theta_p)} \underbrace{(a + z)}_{\bar{a}(x)}, \quad (4)$$

where $(\cdot)^+$ denotes the Moore-Penrose pseudo (MP) inverse and I is an identity matrix. The UKE satisfies (2) by construction and corresponds to (1), for which we shall build a GP model. Next, we introduce three examples, which we use throughout for illustration. Further details can be found in Sec. S6 of the supplementary material and (Udwadia and Kalaba, 2007, p. 120, p. 213).

Ex. 1 (Particle on surface) Consider a particle as illustrated in Fig. 1 with the known mass m sliding along a surface. While the dynamics of the particle are unknown, we want to leverage the surface geometry. The unconstrained acceleration of the particle amounts to $a = M^{-1}[u_1, u_2, u_3 - mg]^T$ with $M^{-1} = \text{diag}(1/m)$, $g = 9.81 \frac{\text{m}}{\text{s}^2}$, and control forces u_i . The mass slides on the surface $q_3 = p_1 q_1^2 + p_2 q_2^2 + p_3 q_1 + p_4 \cos(p_5 q_1)$, with the states and constraint parameters being denoted as $\{q_i, \dot{q}_i\}$ and $\theta_p = [p_1, \dots, p_5]$. The second time-derivative of the constraint yields (2) as

$$\underbrace{[2p_1 q_1 + p_3 - p_4 p_5 \sin(p_5 q_1), \quad 2p_2 q_2, \quad -1]}_{A(x, \theta_p)} \ddot{q} = \underbrace{[-2p_1 \dot{q}_1^2 - 2p_2 \dot{q}_2^2 + p_4 p_5^2 \dot{q}_1^2 \cos(p_5 q_1)]}_{b(x, \theta_p)}, \quad (5)$$

In addition to τ_{ideal} resulting from (5), a velocity quadratic damping force $F_z = Mz$ decelerates the mass non-ideally such that $z_i = -a_0(v^2/|v|)\dot{q}_i$, with the translatory velocity $v(x)$ and damping coefficient a_0 . One obtains the system's constrained dynamics by inserting (5) as well as $a(x)$ and $z(x)$ into (4). While θ_p can be readily measured and $\{A, b, M\}$ are obtained from a brief mechanical analysis, modeling F_a and F_z pose a considerable challenge for a plethora of mechanical systems.

Ex. 2 (Unicycle) *The unicycle as depicted in Fig. 2 commonly describes the motion of wheeled robots (Siciliano et al., 2010, p.478). Here, a non-holonomic constraint $\dot{q}_2 = \dot{q}_1 \tan(q_3)$ only allows for instantaneous translation along the line C-G. Further, u_1 and u_2 denote control inputs in direction of C-G and around q_3 , respectively. The system is decelerated in driving direction by F_z . F_z is induced by velocity quadratic damping as detailed in Ex. 1.*

Ex. 3 (Controlled Duffing's Oscillator) *The Duffing's oscillator as depicted in Fig. 3 models the behavior of two masses that are subject to cubic spring forces and liner damping. An external control force imposes the constraint $q_2 = q_1 + p_1 \exp(-p_2 t) \sin(p_3 t)$. The uncontrolled system is defined as the unconstrained system such that F_a origins from spring and damping forces.*

5. A Gaussian Process Model for Learning Constrained Dynamics

In this section, a constrained GP is derived from the UKE formulation of constrained mechanics in Section 4. To this end, we leverage that GPs are closed under linear transformations and that the operators underlying the UKE are projections. Thus, we obtain a transformed GP model for learning constrained dynamics whose mean and samples fulfill Gauss' principle.

5.1. Gaussian Process Regression

We consider learning of h in (1) with GP regression. Specifically, we approximate the true dynamics h with a multi-output GP \hat{h} (Alvarez et al., 2012), $\hat{h}(x) \sim \mathcal{GP}(\mu(x), K(x, x'))$ where $\mu : \mathbb{R}^D \rightarrow \mathbb{R}^n$ denotes the prior function mean, $\mu(x) = \mathbb{E}[h(x)]$, and $K(x, x') : \mathbb{R}^{D \times D} \rightarrow \mathbb{R}^{n \times n}$ the prior covariance, $K(x, x') \triangleq K_{x, x'} = \mathbb{E}[(h(x) - \mu(x))(h(x') - \mu(x'))^\top]$. Given a GP model, predictions of $\hat{h}(x_*)$ are made – at a point x_* using observations y at inputs X – by computation of the covariance matrices $K(x_*, X)$ and $K(X, X)$ and conditioning the GP via

$$\mu_{x_*|X, y} = \mu_{x_*} + K_{x_*, X}(K_{X, X} + \sigma_y^2 I)^{-1}(y - \mu_X), \quad (6)$$

$$K_{x_*|X, y} = K_{x_*, x_*} - K_{x_*, X}(K_{X, X} + \sigma_y^2 I)^{-1}K_{X, x_*}^\top. \quad (7)$$

5.2. Gauss Principle adhering Gaussian Processes

The UKE (4) disentangles the acceleration $\ddot{q}(x)$ into a term that results from the unconstrained acceleration (being transformed), $T(x)a(x)$, one that is caused from the ideal part of the constraints (2), $L(x)b(x)$, and one caused by the non-ideal part of the constraints, $T(x)z(x)$. Hence, it provides the structure to build the sought GP model. The second term is known from the structural knowledge $A(x, \theta_p)$, $b(x, \theta_p)$, and $M(x, \theta_p)$, while on the other terms, we will place a GP prior. More specifically, we consider two cases of prior structural knowledge: (i) knowing the true $\theta_p = \theta_p^*$, or (ii) knowing only the functional form of $A(x, \theta_p)$, $b(x, \theta_p)$, $M(x, \theta_p)$, but not the true parameters θ_p^* . While we omit the dependencies on θ_p to ease the notation in the following, our work addresses both cases. As for case (ii), θ_p will be treated as additional hyperparameters of the model.

We propose to model the unconstrained acceleration and non-ideal constraining acceleration jointly by placing a GP prior on $\bar{a}(x)$ such that $\hat{\bar{a}} \sim \mathcal{GP}(\mu_{\bar{a}}(x), K_{\bar{a}}(x, x'))$. As GPs are closed under linear transformations, inserting $\hat{\bar{a}}$ into (4) results in a GP modeling $\ddot{q}(x)$ as

$$\hat{h} \sim \mathcal{GP}(L(x)b(x) + T(x)\mu_{\bar{a}}(x), T(x)K_{\bar{a}}(x, x')T(x')^\top). \quad (8)$$

To the above model, we refer to as a *Gauss' Principle adhering Gaussian Process* (GP²). By construction, the GP²'s predictions (mean and samples) satisfy (2). We further note the following favorable properties of the proposed model.

Flexible model. If no prior knowledge about the unconstrained dynamics is available $\mu_{\bar{a}}(x)$ can be set to be the null vector. Alternatively, if a prior model for the unconstrained dynamics is known, this knowledge can be incorporated in form of the mean function $\mu_{\bar{a}}(x)$ in (8). This in return implies that $K_{\bar{a}}(x, x')$ solely models the non-ideal part of the constraint forces plus the residuals of the parametric model. For example, in Ex. 2, the functional structure of $a(x, \theta_p)$ is oftentimes known a priori. In this case, one can set $\mu_{\bar{a}}(x) = a(x, \theta_p)$. As we show in the experimental section, the parameters describing $\mu_{\bar{a}}(x)$ can then be estimated alongside the parameters of $K_{\bar{a}}(x, x')$.

Inferring the unconstrained acceleration alongside. As the constrained GP results from a linear transformation of $\bar{a}(x)$, the joint distribution is obtained as

$$\begin{bmatrix} \hat{\bar{a}} \\ \hat{h} \end{bmatrix} \sim \mathcal{GP} \left(\begin{bmatrix} \mu_{\bar{a}}(x) \\ \mu_{\hat{h}}(x) \end{bmatrix}, \begin{bmatrix} K_{\bar{a}}(x, x') & K_{\bar{a}}(x)T(x')^\top \\ T(x)K_{\bar{a}}(x, x') & T(x)K_{\bar{a}}(x, x')T(x')^\top \end{bmatrix} \right). \quad (9)$$

That is, with (6) one can directly infer $\bar{a}(x)$ from data of the constrained system, as well as condition the constrained acceleration $\hat{h}(x)$ on prior knowledge of $\bar{a}(x)$.

Knowledge transfer between constraint configurations. In many systems, altering the constraint configuration $\{A(x, \theta_p), b(x, \theta_p)\}$ to a different known configuration $\{A'(x, \theta'_p), b'(x, \theta'_p)\}$ does not change $\{\bar{a}, M\}$. For example, imagine taking a mass particle (Ex. 1) from one shape of surface to a different one with the same tribological properties. In this case, it is possible to transfer knowledge in form of \mathcal{D} from one system to the different system using the joint distribution

$$\begin{bmatrix} \hat{h} \\ \hat{h}' \end{bmatrix} \sim \mathcal{GP} \left(\begin{bmatrix} \mu_{\hat{h}}(x|\theta_p) \\ \mu_{\hat{h}'}(x|\theta'_p) \end{bmatrix}, \begin{bmatrix} T(x|\theta_p)K_{\bar{a}}(x, x')T(x'|\theta_p)^\top & T(x|\theta_p)K_{\bar{a}}(x, x')T'(x'|\theta'_p)^\top \\ T'(x|\theta'_p)K_{\bar{a}}(x, x')T(x'|\theta_p)^\top & T'(x|\theta'_p)K_{\bar{a}}(x, x')T'(x'|\theta'_p)^\top \end{bmatrix} \right). \quad (10)$$

6. Experimental Results

In this section, the properties of the proposed GP² model are analyzed on the benchmark systems detailed in Ex. 1 to 3. We compare the GP² to standard (multi-output) GPs.¹

The system parameters are detailed in Sec. S6 of the supplementary material. The input training data consists of randomly sampled observations lying inside the constrained state space. The training data was generated using the analytic ODE (1). The prediction points originate from an equidistant discretization of the constrained state-space. The training data is normalized to have zero mean and standard deviation of one.

As a first baseline for model comparison, the individual \ddot{q}_i are modelled independently as $\ddot{q}_i \sim \mathcal{GP}(0, k_{\text{SE}}(x, x'))$, with squared exponential (SE) covariance function $k_{\text{SE}}(x, x')$. Further, we compare to a standard multi-output GP model, the (GPy, 2012) implementation of the LMC (Alvarez et al., 2012) with matrix $B_i = W_i W_i^\top + I_n \kappa$, $W_i \in \mathbb{R}^{n \times r}$, and $\kappa > 0$, reading $K(x, x') = B_1 k_{\text{SE}}(x, x') + B_2 k_{\text{bias}}(x, x') + B_3 k_{\text{linear}}(x, x')$. Inhere, k_{linear} and k_{bias} denote a linear and bias covariance function respectively (Rasmussen and Williams, 2006). The model $K(x, x') = B_1 k_{\text{SE}}(x, x')$ is referred to as ICM. The hyperparameters are optimized by maximum likelihood estimation via

1. The simulation code is available on: https://github.com/AndReGeist/gp_squared

Table 1: Comparison of the normalized GPs' predicted mean RMSE, and maximum constraint error for 10 runs. For the RMSE, the mean, min. (subscript) and max. (superscript) values are shown.

	RMSE			max. constraint error		
	Surface	Unicycle	Duffing	Surface	Unicycle	Duffing
Analy. ODE	—	—	—	$2 \cdot 10^{-15}$	$6 \cdot 10^{-17}$	$2 \cdot 10^{-14}$
SE	.235 ^{.272} _{.190}	0.27 ^{0.40} _{0.20}	.011 ^{.033} _{.004}	2.6	0.22	6.4
ICM	.244 ^{.277} _{.223}	0.21 ^{0.27} _{0.15}	.003 ^{.005} _{.002}	1.5	0.22	0.5
LMC	.194 ^{.233} _{.159}	0.21 ^{0.28} _{0.15}	.003 ^{.006} _{.001}	1.8	0.26	0.023
GP ² , $\theta_p = \theta_p^*$, $\mu_{\bar{a}} = 0$.058 ^{.066} _{.045}	0.10 ^{0.20} _{0.06}	.007 ^{.019} _{.001}	$4 \cdot 10^{-12}$	$2 \cdot 10^{-12}$	$1 \cdot 10^{-8}$
GP ² , $\theta_p = \theta_p^*$, $\mu_{\bar{a}} \neq 0$.023 ^{.032} _{.018}	0.08 ^{0.15} _{0.05}	.005 ^{.029} _{.002}	$1 \cdot 10^{-13}$	$6 \cdot 10^{-13}$	$3 \cdot 10^{-8}$
GP ² , est. θ_p , $\mu_{\bar{a}} = 0$.065 ^{.071} _{.056}	0.13 ^{0.30} _{0.05}	.009 ^{.028} _{.003}	0.12	$9 \cdot 10^{-13}$	0.013
GP ² , est. θ_p , $\mu_{\bar{a}} \neq 0$.027 ^{.037} _{.020}	0.12 ^{0.20} _{0.06}	.020 ^{.077} _{.004}	0.09	$9 \cdot 10^{-13}$	0.006

L-BFGS-b (Zhu et al., 1997). For the GP², we model $\bar{a} \sim \mathcal{GP}(0, k_{\text{SE}}(x, x'))$, see also Sec. S2 of the supplementary material, with the same optimization settings as for the other models. For $\mu_{\bar{a}} \neq 0$, the prior mean of \bar{a} is set to $\mu_{\bar{a}} = a(x, \theta_p)$ for Ex. 1 and 2, while for Ex. 3 $\mu_{\bar{a}}$ models the linear part of the acceleration induced by dampers and springs. Here, the spring and damping parameters are added to θ_p and estimated alongside the other parameters.

Optimization and prediction In each of 10 optimization runs, 100 observations are sampled while the optimization is restarted 30 times for the benchmark GPs and five times for the GP² model. The prediction results after optimization are depicted in Table 1. For the mechanically constrained systems of Ex. 1 and 2, the GP² shows improved prediction accuracy. The performance can be further increased via the incorporation of additional structural knowledge in form of $\mu_{\bar{a}}$ ($\mu_{\bar{a}} \neq 0$ in Table 1). If θ_p is estimated (est. θ_p) the constraint error increases. For Ex. 1 and 3, θ_p was estimated accurately, whereas the unicycle's parameters (I_c, R) converged to their correct ratio. In the case of Ex. 3, a controller constrains the two masses to oscillate synchronously over time. Unlike the unconstrained dynamics that show nonlinear oscillatory behavior, the constrained system dynamics move similar to a single linearly damped oscillator. In this scenario, the GP² compares less favorable to the other models as it is learning on the more complex unconstrained dynamics. For all examples, the GP² demonstrates a considerable improvement with regards to constraint satisfaction.

Extrapolation and transfer For illustration of the prediction characteristics, we assume the constraint parameters as given and estimated the remaining GP's hyperparameters on 200 observations. Figure 4a illustrates that the GP² model *extrapolates* the prediction result for Ex. 1 ($v = 0$). Yet, extrapolation requires $\bar{a}(X) = \bar{a}(x^*)$. This is not the case for velocity input dimensions when damping plays a predominant role. For a different surface $q_3 = 0.1q_1 - 0.15q_2 - 0.1 \cos(3q_1)$ resulting in $\hat{h}'(x)$ and with $\bar{a}(x) = \bar{a}'(x)$, (10) enables the transfer of the knowledge inherent in $y(x)$ to $\hat{h}'(x)$. Figure 4b (top) illustrates how the GP²'s samples of $\ddot{q}_1(x)$ at $q_3 = 90^\circ$ and $q_3 = -90^\circ$ are forced to zero as the unicycle can only translate in driving direction. Figure Fig. 4b (bottom), shows the posterior distribution $\bar{a}|y$ using (9). For Ex. 1 with $v = 0$ and $u = 0$, \bar{a}_3 is simply $g = 9.81 \frac{m}{s^2}$. For Ex. 2 with $u = 0$, \bar{a} solely consists of a damping force that increases with the translatory velocity.

Trajectory prediction Figure 4c illustrates trajectory predictions on Ex. 1 computed by a Runge-Kutta-45 (RK45) ODE solver. The solver uses either (1), the SE model, or the GP² model. While the

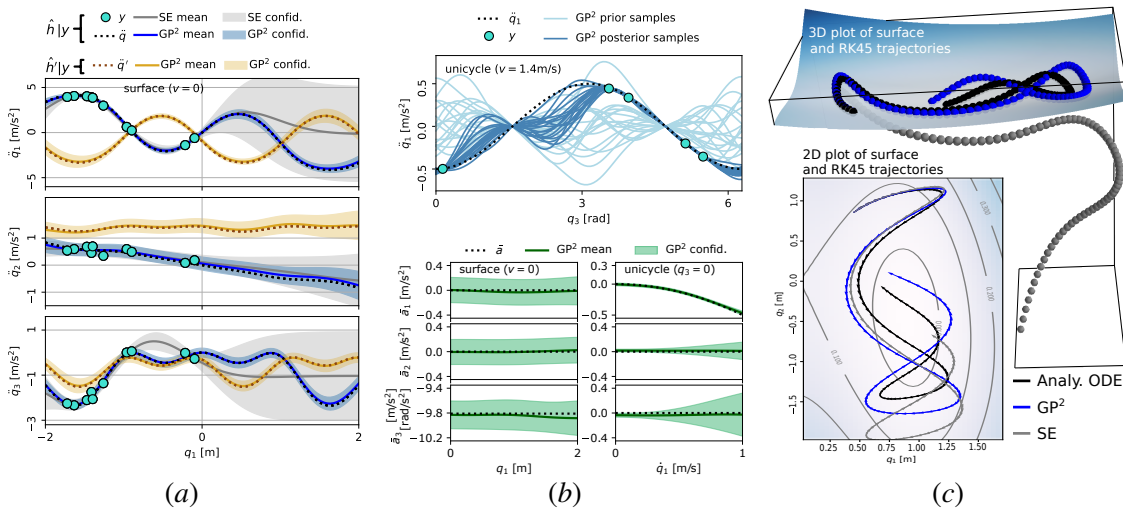


Figure 4: GP² predictions. Figure 4a: Given y from one surface (blue), predictions of \hat{q} on the same and \hat{q}' on another surface (yellow). Figure 4b: (Top) Samples of \hat{h} before and after conditioning on data y ; (Bottom) Prediction of $\hat{a}|y$. Figure 4c: RK45 trajectory predictions of Ex. 1.

SE trajectory prediction leaves the surface, the GP²'s prediction remains on the surface independent of the overall prediction performance. Inhere, the GP² predictions' Euclidean error to the surface increases in the same order of magnitude as with the analytical ODE. In Sec. S7 of the supplementary material, we illustrate that the trajectory predictions of the GP² with estimated hyper-parameters also show improved constraint integrity.

7. Concluding Remarks

We propose a new GP model for learning Lagrangian dynamics that are subject to a non-ideal equality constraint. We leverage that the constraint equation and the system's mass matrix are often straightforward to obtain from a prior mechanical analysis while the constrained dynamics – with non-ideal forces acting on the system – require considerable effort to be modeled parametrically. For typical mechanical examples, the numerical results demonstrate improved data efficiency and constraint satisfaction. While the numerical results herein treat low-dimensional examples chosen for the purpose of illustration, the method also applies when several constraints act onto the system. Investigating the model's benefits on high-dimensional and hardware experiments is subject of ongoing work, and likewise further analysis of the cases of a singular $M(x)$.

Acknowledgments

The authors thank F. Solowjow, A. von Rohr, H. Haresamudram, and C. Fiedler for the helpful discussions. We further thank the Cyber Valley Initiative and the international Max Planck research school for intelligent systems (IMPRS-IS) for supporting A. René Geist.

References

- Christian Agrell. Gaussian processes with linear operator inequality constraints. *Journal of Machine Learning Research*, 20:1–36, 2019.
- Mauricio Alvarez, David Luengo, and Neil D Lawrence. Latent force models. In *Artificial Intelligence and Statistics*, pages 9–16, 2009.
- Mauricio A Alvarez, Lorenzo Rosasco, Neil D Lawrence, et al. Kernels for vector-valued functions: A review. *Foundations and Trends in Machine Learning*, 4(3):195–266, 2012.
- Roberto Calandra, Jan Peters, Carl Edward Rasmussen, and Marc Peter Deisenroth. Manifold Gaussian processes for regression. In *International Joint Conference on Neural Networks (IJCNN)*, pages 3338–3345. IEEE, 2016.
- Ching-An Cheng and Han-Pang Huang. Learn the Lagrangian: A vector-valued rkhs approach to identifying lagrangian systems. *Transactions on cybernetics*, 46(12):3247–3258, 2015.
- Andreas Doerr, Christian Daniel, Duy Nguyen-Tuong, Alonso Marco, Stefan Schaal, Marc Toussaint, and Sebastian Trimpe. Optimizing long-term predictions for model-based policy search. In *Conference on Robot Learning*, pages 227–238, 2017.
- Andreas Doerr, Christian Daniel, Martin Schiegg, Nguyen-Tuong Duy, Stefan Schaal, Marc Toussaint, and Trimpe Sebastian. Probabilistic recurrent state-space models. volume 80 of *Proceedings of Machine Learning Research*, pages 1280–1289, Stockholm Sweden, 10–15 Jul 2018. PMLR.
- Stefanos Eleftheriadis, Tom Nicholson, Marc Deisenroth, and James Hensman. Identification of Gaussian process state space models. In *Advances in neural information processing systems*, pages 5309–5319, 2017.
- Roger Frigola, Fredrik Lindsten, Thomas B Schön, and Carl Edward Rasmussen. Bayesian inference and learning in Gaussian process state-space models with particle MCMC. In *Advances in Neural Information Processing Systems*, pages 3156–3164, 2013.
- Carl Friedrich Gauß. Über ein neues allgemeines Grundgesetz der Mechanik. *Journal für die reine und angewandte Mathematik*, 4:232–235, 1829.
- GPpy. GPpy: A Gaussian process framework in python. <http://github.com/SheffieldML/GPy>, 2012.
- Samuel Greydanus, Misko Dzamba, and Jason Yosinski. Hamiltonian neural networks. In *Advances in Neural Information Processing Systems*, pages 15353–15363, 2019.
- Carl Jidling, Niklas Wahlström, Adrian Wills, and Thomas B Schön. Linearly constrained Gaussian processes. In *Advances in Neural Information Processing Systems*, pages 1215–1224, 2017.
- Juš Kocijan, Agathe Girard, Blaž Banko, and Roderick Murray-Smith. Dynamic systems identification with Gaussian processes. *Mathematical and Computer Modelling of Dynamical Systems*, 11(4):411–424, 2005.

- Markus Lange-Hegermann. Algorithmic linearly constrained Gaussian processes. In *Advances in Neural Information Processing Systems*, pages 2141–2152, 2018.
- Fernando Díaz Ledezma and Sami Haddadin. Fop networks for learning humanoid body schema and dynamics. In *2018 IEEE-RAS 18th International Conference on Humanoid Robots (Humanoids)*, pages 1–9. IEEE, 2018.
- Michael Lutter, Christian Ritter, and Jan Peters. Deep lagrangian networks: Using physics as model prior for deep learning. 2018.
- César Lincoln C Mattos, Andreas Damianou, Guilherme A Barreto, and Neil D Lawrence. Latent autoregressive Gaussian processes models for robust system identification. *IFAC-PapersOnLine*, 49(7):1121–1126, 2016.
- Duy Nguyen-Tuong and Jan Peters. Using model knowledge for learning inverse dynamics. In *International Conference on Robotics and Automation (ICRA)*, pages 2677–2682. IEEE, 2010.
- Duy Nguyen-Tuong and Jan Peters. Model learning for robot control: a survey. *Cognitive processing*, 12(4):319–340, 2011.
- Carl Edward Rasmussen and Christopher KI Williams. *Gaussian processes for machine learning*. The MIT press, 2006.
- Simo Särkkä. Linear operators and stochastic partial differential equations in Gaussian process regression. In *International Conference on Artificial Neural Networks*, pages 151–158. Springer, 2011.
- Bruno Siciliano, Lorenzo Sciavicco, Luigi Villani, and Giuseppe Oriolo. *Robotics: modelling, planning and control*. Springer Science & Business Media, 2010.
- Ercan Solak, Roderick Murray-Smith, William E Leithead, Douglas J Leith, and Carl E Rasmussen. Derivative observations in Gaussian process models of dynamic systems. In *Advances in neural information processing systems*, pages 1057–1064, 2003.
- Firdaus E Udwadia and Robert Kalaba. *Analytical dynamics: a new approach*. Cambridge University Press, 2007.
- Firdaus E Udwadia and Robert E Kalaba. A new perspective on constrained motion. *Proceedings of the Royal Society of London. Series A: Mathematical and Physical Sciences*, 439(1906):407–410, 1992.
- Firdaus E Udwadia and Robert E Kalaba. On the foundations of analytical dynamics. *International Journal of non-linear mechanics*, 37(6):1079–1090, 2002.
- Firdaus E Udwadia, Robert E Kalaba, and Hee-Chang Eun. Equations of motion for constrained mechanical systems and the extended dalemberts principle. *Quarterly of Applied Mathematics*, 55(2):321–331, 1997.
- Ciyou Zhu, Richard H Byrd, Peihuang Lu, and Jorge Nocedal. Algorithm 778: L-bfgs-b: Fortran subroutines for large-scale bound-constrained optimization. *ACM Transactions on Mathematical Software (TOMS)*, 23(4):550–560, 1997.

Supplementary Material: Learning Constrained Dynamics with Gauss' Principle adhering Gaussian Processes

A. René Geist [†]

Sebastian Trimpe [†]

[†] *Intelligent Control Systems Group, Max Planck*

GEIST@IS.MPG.DE

TRIMPE@IS.MPG.DE

On the following pages, several supplementary aspects related to the Udwadia-Kalaba equation (UKE) for non-ideally constrained dynamical systems as well as Gauss' Principle adhering Gaussian Processes (GP²) are discussed.

Section S1 details closedness of Gaussian Processes (GPs) under linear operations. Section S2 provides a description on the implementation of the Gauss' principle adhering Gaussian process (GP²) model. Section S3 gives a brief introduction to the role of constraint equations in classical mechanics. Section S4 sketches the derivation of the Udwadia-Kalaba equation for non-ideally constrained systems. Section S5 briefly discusses the case of having a singular mass matrix in the unconstrained equation of motion. Section S6 provides further details on the unicycle system (Example 2) and the controlled Duffing's oscillator system (Example 3). Section S7 further discusses the trajectory prediction results shown in Figure 4.c of the main manuscript.

S1. Gaussian Process under Linear Operations

While Gaussian distributions are closed under linear transformations, Gaussian processes are closed under linear operations (Rasmussen and Williams, 2006). By applying a functional \mathcal{A}_x on both the mean and covariance function of a GP, its transformed prior distribution is given by

$$\mathcal{A}_x f \sim \mathcal{GP}(\mathcal{A}_x \mu(x), \text{Cov}[\mathcal{A}_x f(x), \mathcal{A}_{x'} f(x')]), \quad (1)$$

with the transformed covariance matrix reading

$$\begin{aligned} \text{Cov}[\mathcal{A}_x f(x), \mathcal{A}_{x'} f(x')] &= \mathbb{E} \left[(\mathcal{A}_x f(x) - \mathcal{A}_x \mu(x)) (\mathcal{A}_{x'} f(x') - \mathcal{A}_{x'} \mu(x'))^\top \right] \\ &= \mathcal{A}_x \mathbb{E} \left[(f(x) - \mu(x)) (f(x') - \mu(x'))^\top \right] \mathcal{A}_{x'}^\top \\ &= \mathcal{A}_x K(x, x') \mathcal{A}_{x'}^\top. \end{aligned} \quad (2)$$

Note that for the transformed GP to exist, the covariance function $K(x, x')$ must be well defined under the operator \mathcal{A}_x . For example if \mathcal{A}_x is a differential operator, then $K(x, x')$ must be a differentiable function. In the Gauss Principle adhering Gaussian Process (GP²) model, the functionals transforming the GP are projection matrices and therefore do not impose additional requirements on the mean and covariance function of the untransformed GP.

S2. Implementation of GP²

To implement the GP² model, $K_{\bar{a}}(x, x')$ must be chosen. The mean and covariance of the GP² model are then obtained after point-wise transformation of $K_{\bar{a}}(x, x')$ at $\{x_k, x'_k\}$ using $\{A, b, M\}$.

With this, standard GP regression and hyperparameter optimization can be performed. If A is a non-zero row-vector then the computation of the MP-inverse reduces to $A^+ = A^T/(AA^T)$, whereas if $m > 1$, (Udwadia and Kalaba, 2007, p. 51) suggests a recursive scheme (Greville, 1960) to compute A^+ . Note that in our implementation, we scaled the outputs of the GP² model using the empirical mean vector μ_s and diagonal scaling matrix S containing the standard deviations $\sigma_{s,i}$ of the training observation vectors $y_k, k = 1, \dots, N$, such that

$$\hat{h}_s \sim \mathcal{GP}(S^{-1}(\mu_{\hat{h}} - \mu_s), S^{-1}k_{\hat{h}}(x, x')(S^{-1})^T). \quad (3)$$

S3. Virtual Displacements and D'Alembert's Principle

Virtual displacements and D'Alembert's Principle are central to understanding the intricacies of constrained motion in mechanical systems. D'Alembert's Principle forms the base for the derivations of all descriptions of constrained dynamical systems in classical mechanics. We mostly omit the arguments of the various functions for the sake of brevity.

Assume that the configuration of a system of rigid bodies is described by the generalized coordinate n -vector $q(t)$. The unconstrained motion of the system is expressed by a second-order ODE of the form

$$a(q, \dot{q}, t) = M^{-1}(q, t)^{-1}F_a(q, \dot{q}, t), \quad (4)$$

where $F_a(q, \dot{q}, t)$ denotes an impressed force and $M(q, t)$ a positive-definite and symmetric matrix. Constraints apply an additional force $F_c(q, \dot{q}, t)$ onto the system as a reaction to its current configuration such that the constrained motion of the system is described by

$$\ddot{q} = h(q, \dot{q}, t) = M^{-1}(q, t)(F_a(q, \dot{q}, t) + F_c(q, \dot{q}, t)). \quad (5)$$

The constraining equation is obtained after differentiating the (non-)holonomic constraint equations (twice) with respect to time such that they take the form

$$A(q, \dot{q}, t)\ddot{q} = b(q, \dot{q}, t). \quad (6)$$

A virtual displacement δq denotes the difference between the current displacement at time t and a possible displacement at the *same* time t (Udwadia and Kalaba, 2007, p. 133). The concept of virtual displacements is of enormous importance for classical mechanics as many mechanical constraints impress *solely* constraint forces onto the system such that

$$\delta q^T F_{c,\text{ideal}} = 0. \quad (7)$$

That is the work of these constraint forces is zero under virtual displacements. Equation (7) is referred to as the D'Alembert(-Lagrange)'s principle (d'Alembert, 1743; Lagrange, 1787). Udwadia et al. (1997) extended the discussion on what constitutes a virtual displacement. After analyzing the possible displacement of the constrained system at time t via a Taylor series expansion they concluded that the virtual displacement δq fulfills

$$A(q, \dot{q}, t)\delta q = 0. \quad (8)$$

With (7) and the definition of δq as in (8), this extended D'Alembert's principle highlights that $F_{c,\text{ideal}} \in \mathcal{R}(A)$, with $\mathcal{R}(A)$ denoting the range space of A .

In many mechanical systems the constraint forces F_c do work. Therefore, (Udwadia and Kalaba, 2000) proposes a generalization of D'Alembert's principle such that

$$\delta q^T F_c = \delta q^T F_{c,\text{nonideal}}, \quad (9)$$

where $F_{c,\text{nonideal}} \hat{=} F_z$ denotes the part of $F_c = F_{c,\text{ideal}} + F_{c,\text{nonideal}}$ that is coaxial to δq . With (8), the generalization of D'Alembert's principle states that in addition to $F_{c,\text{ideal}}$, F_c contains a nonideal part $F_z \in \mathcal{N}(A)$, with $\mathcal{N}(A)$ denoting the null space of A .

S4. Udwadia Kalaba Equation with Non-ideal Constraints

The equation of motion for a system being subject to non-ideal constraints is derived in Udwadia and Kalaba (2002). In this derivation the matrix factorization $M^{1/2} = W\Lambda^{1/2}W^T$ with $\Lambda = \text{Diag}(\lambda_1^{1/2}, \dots, \lambda_n^{1/2})$ and $\lambda_i^{1/2}$ being the i -th eigenvalue of M and W containing the eigenvectors of M is used to scale the acceleration of the system such that $\ddot{q}^s = M^{1/2}\ddot{q}$, $a^s = M^{1/2}a$, and $\ddot{q}_c^s = M^{1/2}\ddot{q}_c = M^{-1/2}F_c$. In return the scaled constraining equation (6) reads

$$AM^{-1/2}M^{1/2}\ddot{q} = B\ddot{q}^s = b, \quad (10)$$

and hence the constrained acceleration can be described by the orthogonal decomposition

$$\ddot{q}^s = (B^+B)\ddot{q}^s + (I - B^+B)\ddot{q}^s. \quad (11)$$

Inserting (5) and (10) into (11) yields

$$\ddot{q}^s = B^+b + (I - B^+B)(a^s + \ddot{q}_c^s). \quad (12)$$

From (12) it follows that \ddot{q}_c^s is given by

$$\ddot{q}_c^s = B^+(b - Ba^s) + (I - B^+B)\ddot{q}_c^s, \quad (13)$$

From (9) it follows that the only part of \ddot{q}_c^s that lies in $\mathcal{N}(B)$ is $z^s = M^{-1/2}F_z$, and hence

$$\ddot{q}_c^s = B^+(b - Ba^s) + (I - B^+B)z^s. \quad (14)$$

By use of $B^+ = B^T(BB^T)^+ = (B^TB)^+B^T$ and (14) inserted into (12) the UKE for a nonideally constrained system is given by

$$\begin{aligned} \ddot{q} &= a + M^{-1/2}B^+(b - Aa) + M^{-1/2}(I - B^+B)z^s, \\ &= M^{-1}A^T(AM^{-1}A^T)^+b + (I - M^{-1}A^T(AM^{-1}A^T)^+A)(a + z). \end{aligned} \quad (15)$$

S5. More on the Rank of the Constraining and Mass Matrices

In this work, we assumed that the mass matrix M of the dynamical system is positive definite.

If the unconstrained acceleration (4) is described by a minimum number of coordinates the Lagrange equations yield a positive definite M . While it is in general possible to describe the motion of a mechanical system using a minimum number of coordinates, it can be more practical for the derivation of the unconstrained equation of motion to use more than the minimum number of coordinates. However, this would then result in a singular mass-matrix such that the inverses $M^{-1/2}$ and M^{-1} do not exist and hence (15) is not well defined. Note that Udwadia and Wanichanon (2013) propose an extension of the UKE for nonideal constraint systems with a singular mass matrix.

S6. Details on the Dynamical Systems of Example 2 and 3

In this section, we further discuss the unicycle and Duffing's oscillator dynamical systems introduced in the experimental results section of the paper. The derivation of these systems is further detailed in (Udwadia and Kalaba, 2007, p. 120, 213).

In general, the functions of the constraining equation $\{A, b\}$ are straightforwardly obtained by a prior kinematic analysis in which first the constraint equations are derived and then differentiated with respect to time. The parameters of the constraining equations can be estimated alongside the GP's parameters. The inertia matrix M is obtained by a rigid body dynamic analysis without the need to consider any induced forces, as these shall be inferred by a GP.

The individual components of the dynamical equations of the unicycle and Duffing's oscillator are depicted in Table 1. The constrained dynamics function of these systems is obtained by inserting the functions in Table 1 together with the non-ideal constraint forces F_z into the UKE.

Fig. 1 to 4 depict the positions and accelerations of the unconstrained as well constrained Duffing's oscillator starting from the initial position $\{q_1(0) = 1, q_2(0) = 1, \dot{q}_1(0) = 2\pi + 2, \dot{q}_2(0) = 2\}$.

Table 1: Mechanical functions of the unconstrained system and the imposed constraints.

Unicycle	Duffing's Oscillator
$M = \begin{bmatrix} m & 0 & -mR \sin(q_3) \\ 0 & m & mR \cos(q_3) \\ -mR \sin(q_3) & mR \cos(q_3) & Ic \end{bmatrix}$	$M = \begin{bmatrix} m & 0 \\ 0 & m \end{bmatrix}$
$F_a = \begin{bmatrix} mR\dot{q}_3^2 \cos(q_3) + \cos(q_3)u_1, \\ mR\dot{q}_3^2 \sin(q_3) + \sin(q_3)u_1, \\ u_2 \end{bmatrix}$	$F_a = K \begin{bmatrix} q_1 \\ q_2 \end{bmatrix} + C \begin{bmatrix} \dot{q}_1 \\ \dot{q}_2 \end{bmatrix} + \begin{bmatrix} k_1^{nl}(q_1 - q_2)^3 \\ k_2^{nl}q_2^3 - k_1^{nl}(q_1 - q_2)^3 \end{bmatrix}$ <p>with $K = \begin{bmatrix} k_1 & -k_1 \\ -k_1 & k_1 + k_2 \end{bmatrix}, C = \begin{bmatrix} c_1 & -c_1 \\ -c_1 & c_1 + c_2 \end{bmatrix}$</p>
$A = [\tan(q_3) \cos(q_3)^2 \quad -\cos(q_3)^2 \quad 0]$	$A = [1 \quad -1]$
$b = -\dot{q}_1^2 \dot{q}_3$	$b = -p_1 \exp(-p_2 q_3) (p_3^2 \sin(p_3 q_3) + 2p_2 p_3 \cos(p_3 t) - p_2^2 \sin(p_3 q_3))$

The parameters chosen for the simulation of the system parameters are denoted in Table 2. The subscripts 'min' and 'max' denote the minimum and maximum state space dimension respectively. Note that in case of the Duffing's oscillator with a mechanistic mean function ($\mu_{\theta_p} \neq 0$) the estimated hyperparameters consist of the constraint parameters, the linear stiffness parameters k_i^{lin} , and linear damping parameters c_i^{lin} .

S7. Trajectory Generation with GP²

For further illustration of the RK45 prediction in Figure 4 of the main manuscript, Fig. 5 illustrates different trajectory estimation results using differing prediction models. Note that the GP² model with constraint parameter estimation compares favorable to a squared exponential (SE) GP model.

Table 2: Parameters of the system examples in SI-units.

	Mass on surface	Unicycle	Duffing's oscillator
State space dim.	$\dot{q}_{1,\min} = \dot{q}_{2,\min} = 0,$ $\dot{q}_{1,\max} = \dot{q}_{2,\max} = 1,$ $q_{3,\min} = 0, q_{3,\max} = 2\pi,$ $\dot{q}_{3,\min} = -0.5, \dot{q}_{3,\max} = 0.5$ $u_{1,\min} = -1, u_{1,\max} = 1,$ $u_{2,\min} = -0.5, u_{2,\max} = 0.5$	$\dot{q}_{1,\min} = \dot{q}_{2,\min} = 0,$ $\dot{q}_{1,\max} = \dot{q}_{2,\max} = 1,$ $q_{3,\min} = 0, q_{3,\max} = 2\pi,$ $\dot{q}_{3,\min} = -0.5, \dot{q}_{3,\max} = 0.5$ $u_{1,\min} = -1, u_{1,\max} = 1,$ $u_{2,\min} = -0.5, u_{2,\max} = 0.5$	$q_{1,\min} = q_{2,\min} = -4,$ $q_{1,\max} = q_{2,\max} = 4,$ $\dot{q}_{1,\min} = \dot{q}_{2,\min} = -5,$ $\dot{q}_{1,\max} = \dot{q}_{2,\max} = 5,$ $t_{\max} = 0, t_{\max} = 5,$
System param.	$m = 3, g = -9.81, a_0 = 0.2,$ $\theta_p = [0.08, 0.05, 0.05, 0.1, 3]$	$m = 1, a_0 = 0.5,$ $R = 0.05, I_c = 0.02,$ $\theta_p = [R, I_c]$	$m_1 = 2, m_2 = 1,$ $k_1^{\text{nl}} = 1, k_2^{\text{nl}} = 2,$ $k_1^{\text{lin}} = 10, k_2^{\text{lin}} = 12,$ $c_1^{\text{lin}} = 0.1, c_2^{\text{lin}} = 0.15,$ $p_1 = 1, p_2 = 0.3, p_3 = 2\pi$

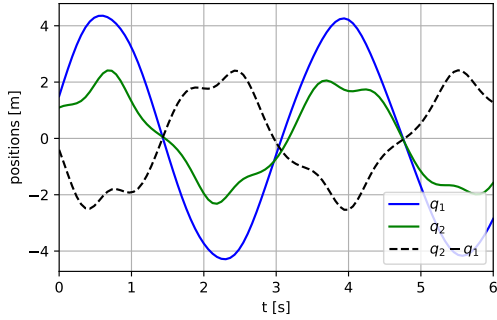


Figure 1: Unconstrained Duffing's oscillator's position plotted over time.

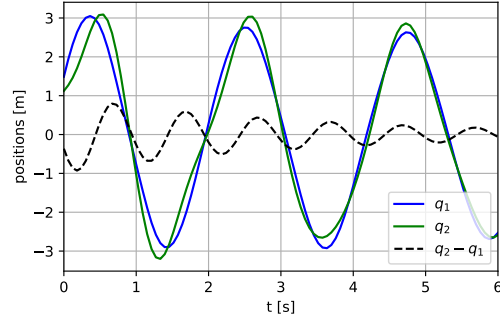


Figure 2: Constrained Duffing's oscillator's position plotted over time.

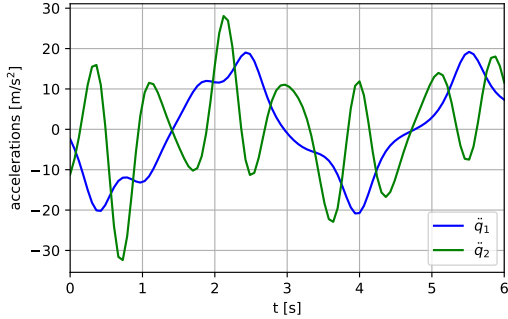


Figure 3: Unconstrained Duffing's oscillator's accelerations plotted over time.

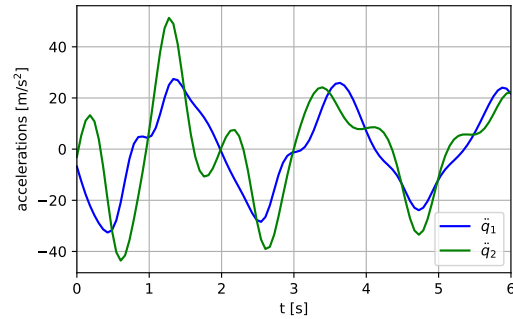


Figure 4: Constrained Duffing's oscillator's accelerations plotted over time.

References

Jean Le Rond d'Alembert. *Traité de dynamique*. 1743.

TNE Greville. Some applications of the pseudoinverse of a matrix. *SIAM review*, 2(1):15–22, 1960.

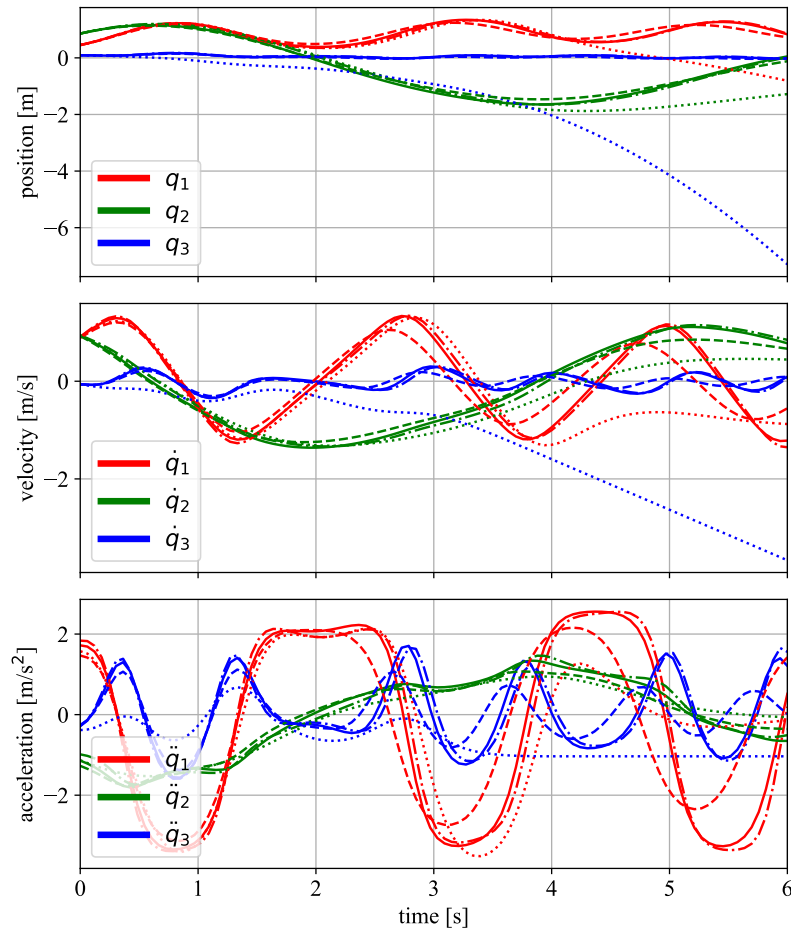


Figure 5: RK45 trajectory predictions of the analytical ODE (---), the SE-GP (···), the GP² with $\theta_p = \theta_p^*$ (—), and GP² with estimated θ_p (-·-)

Joseph Louis Lagrange. *Mécanique analytique*. Mme. De Courcier, Paris, 1787.

Carl Edward Rasmussen and Christopher KI Williams. *Gaussian processes for machine learning*. The MIT press, 2006.

Firdaus E Udwadia and Robert Kalaba. *Analytical dynamics: a new approach*. Cambridge University Press, 2007.

Firdaus E Udwadia and Robert E Kalaba. Nonideal constraints and lagrangian dynamics. *Journal of Aerospace Engineering*, 13(1):17–22, 2000.

Firdaus E Udwadia and Robert E Kalaba. On the foundations of analytical dynamics. *International Journal of non-linear mechanics*, 37(6):1079–1090, 2002.

Firdaus E Udwadia and Thanapat Wanichanon. On general nonlinear constrained mechanical systems. *Numer. Algebra Control Optim*, 3(3):425–443, 2013.

Firdaus E Udwadia, Robert E Kalaba, and Hee-Chang Eun. Equations of motion for constrained mechanical systems and the extended d’alembert’s principle. *Quarterly of Applied Mathematics*, 55(2):321–331, 1997.